Collagen and bone morphogenetic protein-2 functionalized hydroxyapatite scaffolds induce osteogenic differentiation in human adipose-derived stem cells

Nguyen Thuy Ba Linh[1, †], Celine D.G. Abueva[1], Dong-Woo Jang[2] and Byong-Taek Lee[1, *]

[1]Institute of Tissue Regeneration, College of Medicine, Soonchunhyang University, 366-1, Ssangyoungdong, Cheonan-si, Chungnam, 330-090, Republic of Korea

[2]InoBone Corporate R&D Center, Soonchunhyang University, 408 Entrepreneurship, Asan, 336-745, Republic of Korea

[†] Current Address: Eastman Dental Institute, University College London WC1X 8LD, UK

Corresponding Author details:

Prof. Byong-Taek Lee

366-1, Bongmyeong-dong, Cheonan-City, Chungcheongnam-do Soonchunhyang University Hospital, School of Medicine, Room 212, 330-090 Korea

Telephone: 82-41-570-2427; Fax: 82-41-577-2415

E-mail: lbt@sch.ac.kr

ABSTRACT

Surface modification is one important way to fabricate successful biocompatible materials in bone tissue engineering. Hydroxyapatite (HAp) materials have received considerable attention as suitable bioceramics for manufacturing osseous implants due to their similarity to bone mineral in terms of chemical composition. In this study, the surface of porous HAp scaffolds was modified by collagen treatment and bone morphogenetic protein-2 (BMP-2) conjugation. The surface modification did not affect the HAp scaffold's bulk properties. No significant difference in compressive strength was found among different scaffolds, with HAp, collagen modified HAp, and collagen-BMP-2 functionalized HAp having compressive strengths of 45.8 ± 3.12, 51.2 ± 4.09, and 50.7 ± 3.98 MPa, respectively. *In vitro* studies were performed to compare adhesion and osteogenic differentiation between human adipose-derived stem cells (hADSC) with modified surfaces and those unmodified HAp surface. Collagen or BMP-2 alone was insufficient and that both collagen and BMP-2 are necessary to get the desired results. The findings suggest the possibility of using three-dimensional HAp scaffold treated with gold-standard collagen coating and highly researched BMP-2 growth factor as a platform to deliver hADSC. Results of this study could be used to develop treatment strategy for regenerating completely transected models using more synergistic approach.

1. Introduction

To improve biocompatibility and regenerative properties of biomaterials used as bone grafts, modified calcium phosphate-based scaffolds and potent osteoinductive bone morphogenetic proteins (BMPs) have been used.[1-5] However, management of massive segmental bone defects following trauma remains a challenging clinical problem.[6] The aforementioned independent approach might be ineffective in repairing large defects. A synergistic approach might be key to achieve successful bone graft for segmental defects.

Collagen, one of the major components of extracellular matrix (ECM), is secreted by osteoblasts and possesses several important properties for use in bone healing applications.[1] Bone morphogenetic protein-2 (BMP-2) has been clinically applied to expedite spinal fusion and promote the healing of bony non-unions. It has received FDA approval to treat acute tibial fractures.[7] It is administered either in a freely soluble form or mixed with a carrier for loose adsorption. It is administered either in a freely soluble form or mixed with a carrier for loose adsorption. Both have been extensively studied independently or in combination with hydroxyapatite (HAp) for bone regeneration.[8, 9] However, collagen and BMP-2 3D scaffold coating and functionalization for segmental type of defects have not been intensively studied and optimized with no definitive success to date.

Human adipose tissues have shown high potential as a source of mesenchymal stem cells due to their relative abundance compared to other sources such as bone marrow. They have been investigated in combination with carriers or scaffolds for bone tissue engineering applications.[10, 11] Human adipose-derived stem cells (hADSC) have also shown potential to differentiate into adipogenic, osteogenic and chondrogenic lineages.[12, 13] A recent paradigm shift also suggests that stem cells secrete potent combinations of trophic factors that can modulate molecular compositions of the environment and evoke responses from resident cells.[14] Thus, it has become essential to investigate the use of adipose derived mesenchymal

stem cells, its potential towards osteogenic differentiation and commitment, especially in combination with 3D scaffolds. It is also important to observe the effects of collagen and osteogenic factors such as BMP-2 in the differentiation of these adipose derived stem cells. Hence, the objective of this study was to determine hADSC osteogenic differentiation on HAp and modified HAp scaffolds using collagen and BMP-2 for surface modification. This investigation will allow us to determine if surface modification can allow HAp scaffold to serve as a platform capable of supporting hADSC osteogenic differentiation and later as a synergistic approach for regeneration of completely transected bone models with possible clinical application.

2. Materials and Methods

2.1. Materials

Collagen I, bovine serum albumin (BSA), 1-ethyl-3-(3-dimethylaminopropyl)-carbodiimide (EDC), N-Hydroxysuccinimide (NHS), and Glycine were purchased from Sigma-Aldrich (St. Louis, MO, USA). Dimethylsulfoxide 99.0% (DMSO) was purchased from Samchun Pure Chemical Co. Ltd., Korea. Human Adipose Derived Stem Cell (hADSC) and ADSC Growth BulletKit™ were purchased from Lonza Group. Ltd., USA. 3-[4,5-dimethylthiazol-2-yl]-2,5-diphenyltetrazolium bromide (MTT) solution and trypsin-EDTA were purchased from Gibco (Carlsbad, CA, USA). Fluorescein isothiocyanate (FITC)-conjugated phalloidin and Heochst 33342 were from Sigma-Aldrich. Anti-vinculin antibody clone VIIF9 and osteogenesis kit (ARS) were obtained from Merck Millipore (Billerica, MA, USA). Alkaline phosphatase antibody, ALP (H-300), osteopontin, OPN antibody (AKm2A1), BMP-2/4 (H-51) antibody were purchased from Santa Cruz Biotechnology (Dallas, TX, USA).

2.2. Process for collagen modification and rhBMP-2 conjugation

HAp scaffolds were fabricated via multi-extrusion process similar to protocols published previously.[15, 16] For collagen surface modification, HAp porous scaffolds were incubated with 1% w/v bovine serum albumin (BSA) overnight, rinsed twice with distilled water, and then incubated in EDC/NHS cross-linking solution for 1 hour. These scaffolds were incubated overnight in collagen solutions (3 mg/ml). Glycine was added to stop the reaction. These scaffolds were dried in room temperature for 2 hours.

HAp-Collagen scaffolds were conjugated with BMP-2 (10 µg/ml in 1% BSA) at 4 ºC for 24 hours. Scaffolds were then washed with distilled water once to remove excess BMP-2 and air-dried at room temperature for 2 hours. Reaction scheme for collagen surface modification and BMP-2 functionalization is shown in Figure1.

2.3. Structure and chemical analysis of scaffolds

Microstructures of bare HAp, collagen coated (HAp-C) and BMP-2 conjugated (HAp-B) scaffolds were characterized using a scanning electron microscope (SEM, JEOL, JSM-6701F, Japan) coated with platinum (Cressington 108 Auto coater).

Samples were pulverized and subjected to FT-IR imaging and spectroscopic analysis (Nicolet spectrometer system, Nicolet iS10, Thermoscientific). Obtained spectra were analyzed with Omnic Version 7.3 software accompanying the spectrometer over a range of 500–4000 cm^{-1} at a resolution of 8 cm^{-1}.

X-ray photoelectron spectroscopy (XPS, Perkin Elmer PHI 5400) spectra were obtained at passing energy of 70 eV. High-resolution spectra were obtained using a passing energy of 20 eV. All binding energies were referenced to peaks of C1s (carbon) at 281.0 eV.

2.4. Qualitative analysis of BMP-2 by immunofluorescence

Visualization of BMP-2 was performed by incubating scaffolds with BMP-2/4 (H-51) antibody (1:200 Santa Cruz Biotechnology) overnight at 4ºC. These were then incubated with anti-rabbit secondary antibody (Alexa flour 488, 1:1000; Invitrogen). Images were obtained under a

confocal fluorescent microscope (FV10i-W) and analyzed using FV10i-ASW 3.0 viewer software.

2.5. BMP-2 release study

The amount of recombinant human bone morphogenetic protein-2 (rhBMP-2) released at each selected time point (Day 1, 2, 3, 5, 7, 10, 12, 14, 18, and 21) was measured using a BMP-2 Quantikine ELISA Kit (R&D Systems, Inc.) by solid phase sandwich ELISA following the manufacturer's protocols.

2.6. Compressive strength

Compressive strength was determined using a universal testing machine (R&B UNITECH-T, Korea). Samples with dimensions of 5 mm wide × 7 mm long × 7 mm high were prepared. Measurements were taken using a 100 kN load cell. Load deformation data were recorded at a deforming speed of 1 mm/s.

2.7. Cell adhesion behavior

Confocal microscopy was used to observe cell adhesion behavior of hADSC seeded onto HAp, HAp-C and HAp-B scaffolds. Briefly, after 60 and 90 minutes of culture, scaffolds were rinsed with phosphate buffered saline (PBS) twice and fixed in 4% paraformaldehyde (Sigma-Aldrich) for 15 minutes at room temperature. These cells were then permeabilized with 0.25% Triton X-100 (Sigma-Aldrich) for 10 minutes and blocked with 2.5% BSA for 30 minutes. Focal adhesions were visualized by staining with fluorescein isothiocyanate (FITC) conjugated mouse monoclonal anti-vinculin (1:50 dilutions) for 4 hours. F-Actin was labeled by incubating cells with Alexa 564-coupled phalloidin (Molecular Probe, 1:50 dilutions) and for 1 hour. Nuclei were counterstained with Hoechst 33342 (Sigma-Aldrich). Finally these scaffolds were mounted on to glass slides and visualized under confocal fluorescent microscope (Olympus, FV10i-W).

2.8. Cell viability and proliferation

Cell viability and proliferation were observed via confocal microscopy. Approximately 1 x 10^4 hADSC/mL were seeded on HAp, HAp-C, and HAp-B scaffolds. Observations were made after 1, 7, and 14 days of culture. These scaffolds were immunostained with fluorescein isothiocyanate (FITC)-conjugated phalloidin (25 mg/mL). Nuclei were counterstained with Hoechst 33342. Finally, the scaffolds were mounted onto glass slides and visualized under a confocal fluorescent microscope using 10 x and 60 x objectives and the accompanying FV10i-ASW 3.0 Viewer software.

MTT (3-[4, 5-dimethylthiazol-2-yl]-2, 5-diphenyltetrazolium bromide) assay was used to analyze cell viability. Cell viability (OD) of cells cultured on the scaffolds for 1, 7 and 14 days was quantified by adding 100 mL of MTT solution (5 mg/mL in PBS) to each well of a 24-well tissue culture plate. OD values were measured using an ELISA reader (EL, 312, Biokinetics reader; Bio-Tek instruments) at a wavelength of 595 nm.

2.9. Osteogenic differentiation analysis

Osteogenic differentiation of hADSC was performed using human mesenchymal stem cell differentiation medium (Lonza Group. Ltd., USA), following the manufacturer's protocols.

The amount of major extracellular matrix (ECM) secreted by hADSC was qualitatively analyzed using Alizarin red staining (ARS). ARS is a dye that can selectively bind to calcium salts. Hence, it can be used for mineral staining and analysis. After 14 and 21 days, scaffolds seeded with hADSC (1 x 10^6 hADSC/mL) were washed with PBS and fixed with 4% paraformaldehyde for 15 minutes. These constructs were then washed twice with distilled water and stained with 2% ARS for 45 minutes at room temperature. After several washes with distilled water, these scaffolds were observed under an inverted optical microscope. Images were taken using the accompanying image software (Olympus BX51, Tokay, Japan).

Immunocytochemical analysis of alkaline phosphatase and osteopontin (bone-specific protein) was performed by incubating the scaffolds with rabbit anti-alkaline phosphate

antibody (ALP, 1:50, Santa Cruz) and mouse anti-osteopontin antibody (OPN, 1:50, Santa Cruz) overnight at 4ºC. These scaffolds were then incubated with secondary antibody (Alexa flour 488, 1:1000, Invitrogen). Images were visualized under a confocal fluorescent microscope (FV10i-W) using 10x and 60x objectives and the accompanying FV10i-ASW 3.0 Viewer software.

3. Results

3.1. Structure and chemical analysis of scaffolds

Fabricated HAp scaffold photograph (Figure 2 a-b) showed a dense outer shell which gave an ideal structural support to the scaffold together with thin shells present in inner pores. Surface and cross-sectional SEM micrographs of the HAp scaffold's pore network are shown in Figure 2c and 2d, respectively, consisting of 56 pore-channels measured to be approximately 300 µm in diameter.

In this study, BSA that is highly adsorbed on the surface of the HAp scaffold allowed for the easy attachment of collagen via EDC/NHS. In Figure 2e, collagen coating on the scaffold was evident. Fibril formation for collagen can be observed on the surface and fractured area of the HAp-C scaffold, as shown in Figure 2f. Collagen fibers were found to adhere firmly onto the surface of HAp scaffolds indicative of successful collagen coating. Qualitative immunofluorescence analysis of BMP-2 presence (HAp-B) also confirmed successful BMP-2 conjugation onto the modified HAp-C scaffold (Figure 3a).

FT-IR studies were conducted to determine modifications on the scaffold surface. Results are shown in Figure 3b. HAp-B retained characteristic peaks observed for bare HAp with the presence of new peaks for amide II at 1561 cm^{-1} due to collagen and BMP-2's carbonyl group. Peaks of HAp-B were similar to those of HAp-C due to the presence of the same functional group between collagen and BMP-2. XPS spectra (Figure 3c) showed binding energy peaks of

Ca2p, P2s and P2p for HAp scaffold. However, C1s and N1s peaks were found for HAp-C and HAp-B scaffolds, further confirming successful coating and conjugation of collagen and BMP-2 onto HAp scaffolds.

3.2. BMP-2 release profile

Cumulative release profile of BMP-2 is shown in Figure 4a. BMP-2 release was measured at multiple time points. There was an initial burst release of 5.85 ± 2.46% during the first day, followed by a more sustained release in the following days. BMP-2 release was significantly increased at 14 days. This might be due to degradation or hydrolysis of collagen fibers, thus releasing more BMP-2. Most (60.5 ± 4.19%) BMP-2 was released after 21 days. This was also evident in fluorescent stained images of HAp-B showing faint BMP-2 detection (Figure 4b).

3.3. Effect of surface modification on compressive strength of HAp scaffolds

Based on results of compressive strength analysis for bare HAp, HAp-C and HAp-B, the modification processes done did not affect the structural integrity of the scaffolds (Figure 5a). No significant difference ($p<0.05$) in compressive strength was found among different scaffolds, with HAp having a compressive strength of 45.8 ± 3.12 MPa, HAp-C 51.2 ± 4.09 MPa and HAp-B 50.7 ± 3.98 MPa. More in depth analysis also revealed that the inner pore network made of thin shells was weaker. It became compromised or started to break at approximately 36.9 ± 0.55 MPa (Figure 5b).

3.4. Cell adhesion and proliferation behavior

Confocal images of cultured hADSC on HAp scaffold surfaces stained with vinculin for focal adhesion are shown in Figure 6. After 60 minutes of incubation cells were able to adhere to all scaffolds, with more prominent adhesion points for both HAp-C and HAp-B scaffolds. After 90 minutes of incubation, cells on the HAp-B scaffold seemed to show more spreading and flattened morphology, typically corresponding to better attachment of cell actin filaments. The same observation was obtained on the effect of surface modifications on the proliferation of

hADSC cultured on scaffolds based on the SEM and confocal images (Figure 7). Significant difference in cells proliferation was observed at 14 days of culture period for the modified scaffolds compared to unmodified HAp.

3.5. Mineralization, Alkaline phosphatase and Osteopontin analyses

Mineralization assay was performed for hADSC cultured on HAp-C and HAp-B scaffolds followed by Alizarin red staining. Results are shown in Figure 8a. Vast extracellular calcium deposits were found after 21 days of incubation, indicating potential towards osteoblastic differentiation for hADSC cultured on modified scaffolds.

Immunostaining of cells further confirm osteoblastic protein expressions as shown in confocal images (Figure 8b). Primary antibody against ALP was used as early stage marker for bone cell differentiation. Heightened ALP expression was observed for cells cultured on HAp-B scaffold compared to that on HAp-C or HAp scaffold after 14 and 21 days of culture period. Similarly, OPN expression (Figure 9) after 21 days of culture period was more prominent for cells cultured on HAp-B scaffold compared to that on HAp-C or HAp scaffold. These results indicated that HAp-B best supported and promoted the differentiation of cultured hADSC towards osteoblastic lineage compared to unmodified HAp or only collagen modified HAp-C which would also suggest higher ability to enhance bone formation significantly.

4. Discussion

A multipronged approach is necessary to address issues surrounding treatment for load-bearing segmental bone defects. Current strategies focus on a combination of composite hybrid scaffold development and osteoconductive substrates that can deliver osteoinductive growth factors or osteogenic cell sources.[17] We designed a composite hybrid scaffold composed of a ceramic and polymeric material. It could provide sufficient mechanical stability, structure, and calcium source required to serve as a suitable osteoconductive surface for healing segmental

bone defects. Modification by collagen coating and delivery of growth factor BMP-2 were both used in this study to tackle critical-sized defect by attracting cells into the wound environment and onto the scaffold surface, consequently accelerating bone formation. Collagen coating and its positive effects for cell recruitment and bone formation have been well established.[18, 19] Type I collagen is a major structural protein in bone, and collagen coating effectively promotes initial cell attachment.[20, 21] However, collagen coating alone is not sufficient to accelerate the differentiation of osteoblasts.[22] In this regard, it was of interest to investigate the combination of HAp, collagen and BMP-2 and determine whether hADSC proliferation and osteoblastic differentiation would be supported and enhanced. Such potentially synergistic approach for segmental bone regeneration did support more hADSC attachment and proliferation on modified scaffolds HAp-C and HAp-B, with significant difference in hADSC osteogenic differentiation observed for HAp-B. It was also important to note that the modification process did not affect the structural integrity of the fabricated HAp scaffold. Thus, a combination of stable HAp scaffold platform together with collagen coating for improving cell adhesion and conjugation of BMP-2 for enhancing osteobalstic differentiation could be used as a prospective new approach for treating segmental defects.

5. Conclusion

Surfaces of porous HAp scaffolds were modified successfully by collagen and BMP-2. Characteristic evaluation for unmodified and modified scaffolds confirmed that the modification process best supported cell adhesion and proliferation of cultured hADSC. The presence of BMP-2 also significantly enhanced osteogenic differentiation of cultured hADSC. The combination of collagen and BMP-2 are both necessary for successful application of hADSC for bone tissue engineering. Sufficient information was obtained supporting high

potential of HAp-collagen-BMP-2 system as a platform to deliver pre-differentiated hADSC and possible application in a completely transected animal model.

Conflict of Interest

The authors declare no conflicting interests.

Acknowledgement

This research was supported by the Basic Science Research Program through the National Research Foundation of Korea (NRF) funded by the Ministry of Education (2015R1A6A1A03032522) and partially supported by the Soonchunhyang University Research Fund.

References

1. David, F. *et al.* Enhanced bone healing using collagen–hydroxyapatite scaffold implantation in the treatment of a large multiloculated mandibular aneurysmal bone cyst in a thoroughbred filly. *Journal of Tissue Engineering and Regenerative Medicine* 9, 1193-1199, doi:10.1002/term.2006 (2015).
2. Forster, Y. *et al.* Surface modification of implants in long bone. *Biomatter* 2, 149-157 (2012).
3. Liu, X., Rahaman, M. N., Liu, Y., Bal, B. S. & Bonewald, L. F. Enhanced bone regeneration in rat calvarial defects implanted with surface-modified and BMP-loaded bioactive glass (13-93) scaffolds. *Acta biomaterialia* 9, 7506-7517, doi:10.1016/j.actbio.2013.03.039 (2013).

4. Pieske, O. *et al.* Autologous bone graft versus demineralized bone matrix in internal fixation of ununited long bones. *Journal of Trauma Management & Outcomes* 3, 11-11, doi:10.1186/1752-2897-3-11 (2009).
5. Wu, Y., Hou, J., Yin, M., Wang, J. & Liu, C. Enhanced healing of rabbit segmental radius defects with surface-coated calcium phosphate cement/bone morphogenetic protein-2 scaffolds. *Materials Science and Engineering: C* 44, 326-335, doi:http://dx.doi.org/10.1016/j.msec.2014.08.020 (2014).
6. Lin, C.-Y. *et al.* The healing of critical-sized femoral segmental bone defects in rabbits using baculovirus-engineered mesenchymal stem cells. *Biomaterials* 31, 3222-3230, doi:http://dx.doi.org/10.1016/j.biomaterials.2010.01.030 (2010).
7. Gamradt, S. C. & Lieberman, J. R. Genetic Modification of Stem Cells to Enhance Bone Repair. *Annals of Biomedical Engineering* 32, 136-147, doi:10.1023/B:ABME.0000007798.78548.b8.
8. Kikuchi, M. Hydroxyapatite/collagen bone-like nanocomposite. *Biol Pharm Bull* 36, 1666-1669 (2013).
9. Yang, X. & Li, Z. Influence of hydroxyapatite and BMP-2 on bioactivity and bone tissue formation ability of electrospun PLLA nanofibers. *Journal of Applied Polymer Science* 132, n/a-n/a, doi:10.1002/app.42249 (2015).
10. Bodle, J. C., Hanson, A. D. & Loboa, E. G. Adipose-derived stem cells in functional bone tissue engineering: lessons from bone mechanobiology. *Tissue Eng Part B Rev* 17, 195-211 (2011).
11. Dai, R., Wang, Z., Samanipour, R., Koo, K.-i. & Kim, K. Adipose-Derived Stem Cells for Tissue Engineering and Regenerative Medicine Applications. *Stem Cells International* 2016, 19, doi:10.1155/2016/6737345 (2016).

12. de Girolamo, L., Sartori, M. F., Albisetti, W. & Brini, A. T. Osteogenic differentiation of human adipose-derived stem cells: comparison of two different inductive media. *J Tissue Eng Regen Med* 1, 154-157 (2007).
13. Haeri, S. M. J., Sadeghi, Y., Salehi, M., Farahani, R. M. & Mohsen, N. Osteogenic differentiation of human adipose-derived mesenchymal stem cells on gum tragacanth hydrogel. *Biologicals* 44, 123-128, doi:http://dx.doi.org/10.1016/j.biologicals.2016.03.004 (2016).
14. Baraniak, P. R. & McDevitt, T. C. Stem cell paracrine actions and tissue regeneration. *Regenerative medicine* 5, 121-143, doi:10.2217/rme.09.74 (2010).
15. Abueva, C. D. G., Jang, D.-W., Padalhin, A. & Lee, B.-T. Phosphonate-chitosan functionalization of a multi-channel hydroxyapatite scaffold for interfacial implant-bone tissue integration. *Journal of Materials Chemistry B* 5, 1293-1301, doi:10.1039/c6tb03228a (2017).
16. Jang, D.-W., Franco, R. A., Sarkar, S. K. & Lee, B.-T. Fabrication of Porous Hydroxyapatite Scaffolds as Artificial Bone Preform and its Biocompatibility Evaluation. *Asaio Journal* 60, 216-223, doi:10.1097/mat.0000000000000032 (2014).
17. Pilia, M., Guda, T. & Appleford, M. Development of Composite Scaffolds for Load-Bearing Segmental Bone Defects. *BioMed Research International* 2013, 15, doi:10.1155/2013/458253 (2013).
18. Polo-Corrales, L., Latorre-Esteves, M. & Ramirez-Vick, J. E. Scaffold Design for Bone Regeneration. *Journal of nanoscience and nanotechnology* 14, 15-56 (2014).
19. Wojtowicz, A. M. *et al.* Coating of biomaterial scaffolds with the collagen-mimetic peptide GFOGER for bone defect repair. *Biomaterials* 31, 2574-2582 (2010).

20. Cooke, M. J. *et al.* Enhanced cell attachment using a novel cell culture surface presenting functional domains from extracellular matrix proteins. *Cytotechnology* 56, 71-79, doi:10.1007/s10616-007-9119-7 (2008).

21. Somaiah, C. *et al.* Collagen Promotes Higher Adhesion, Survival and Proliferation of Mesenchymal Stem Cells. *PLOS ONE* 10, e0145068, doi:10.1371/journal.pone.0145068 (2015).

22. Wang, T., Yang, X., Qi, X. & Jiang, C. Osteoinduction and proliferation of bone-marrow stromal cells in three-dimensional poly (ε-caprolactone)/ hydroxyapatite/collagen scaffolds. *Journal of Translational Medicine* 13, 152, doi:10.1186/s12967-015-0499-8 (2015).

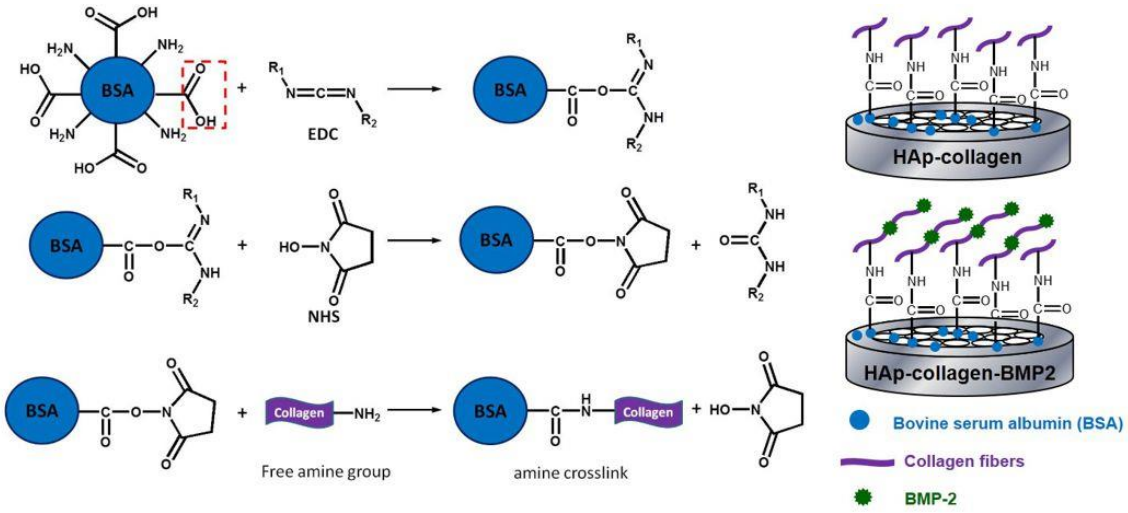

FIGURE 1 Schematic diagram of reaction mechanism involved in the collagen surface modification and BMP-2 functionalization of 3D HAp scaffolds. HAp, hydroxyapatite; BMP, bone morphogenetic protein-2.

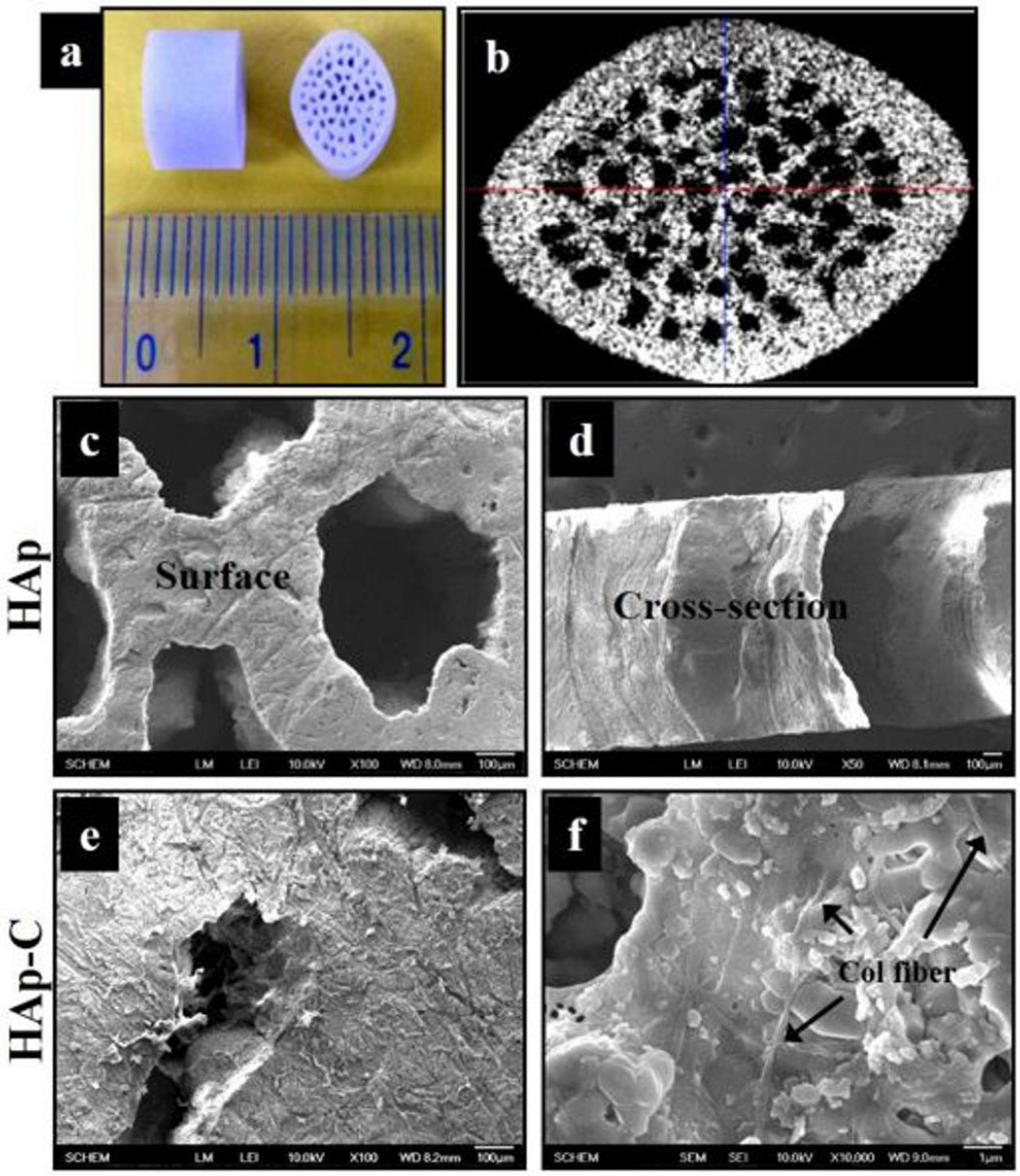

FIGURE 2 (a) Photograph of HAp scaffold with (b) pore structure observed through micro-CT. SEM micrographs of the morphology of the surface of HAp scaffold (c), cross-section (d), and the HAp scaffold coated with collagen (HAp-C) (e,f). HAp, hydroxyapatite; SEM, scanning electron microscopy.

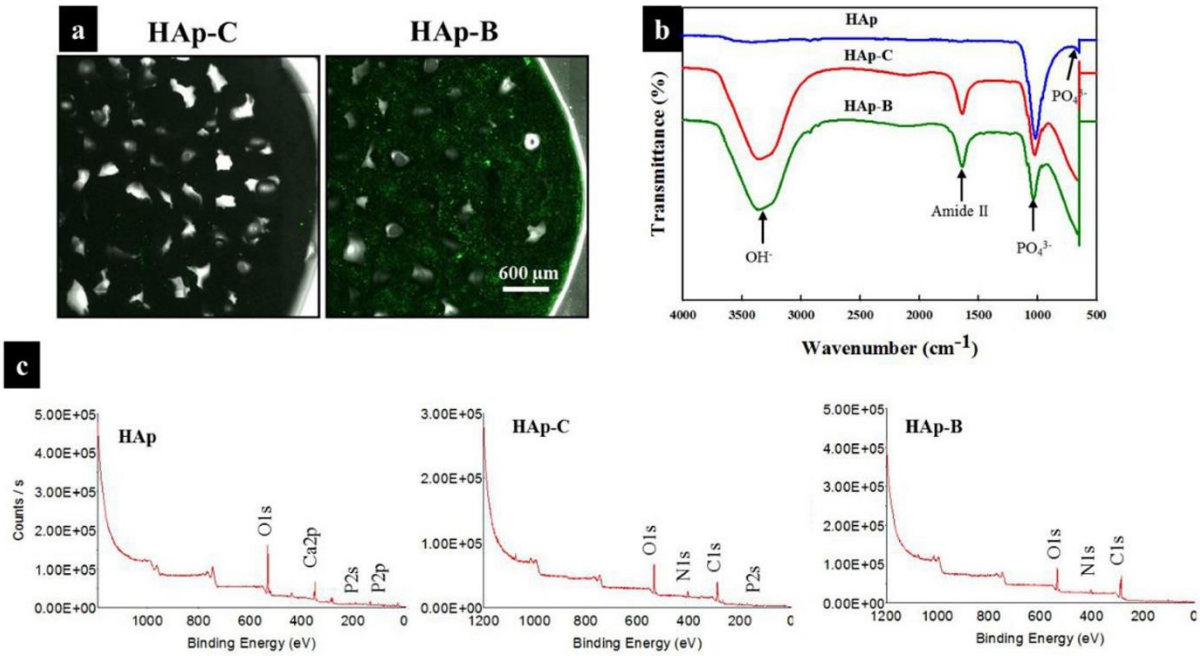

FIGURE 3 Qualitative analyses of BMP-2 attachment on modified scaffold (HAp-C) observed by immunofluorescence staining (BMP-2–FITC) (a), with FT-IR analysis of bare and modified scaffolds (b) and the corresponding XPS spectra (c). BMP-2, bone morphogenetic protein-2; HAp, hydroxyapatite; FITC, fluorescein isothiocyanate; FT-IR, Fourier transform infrared spectroscopy.

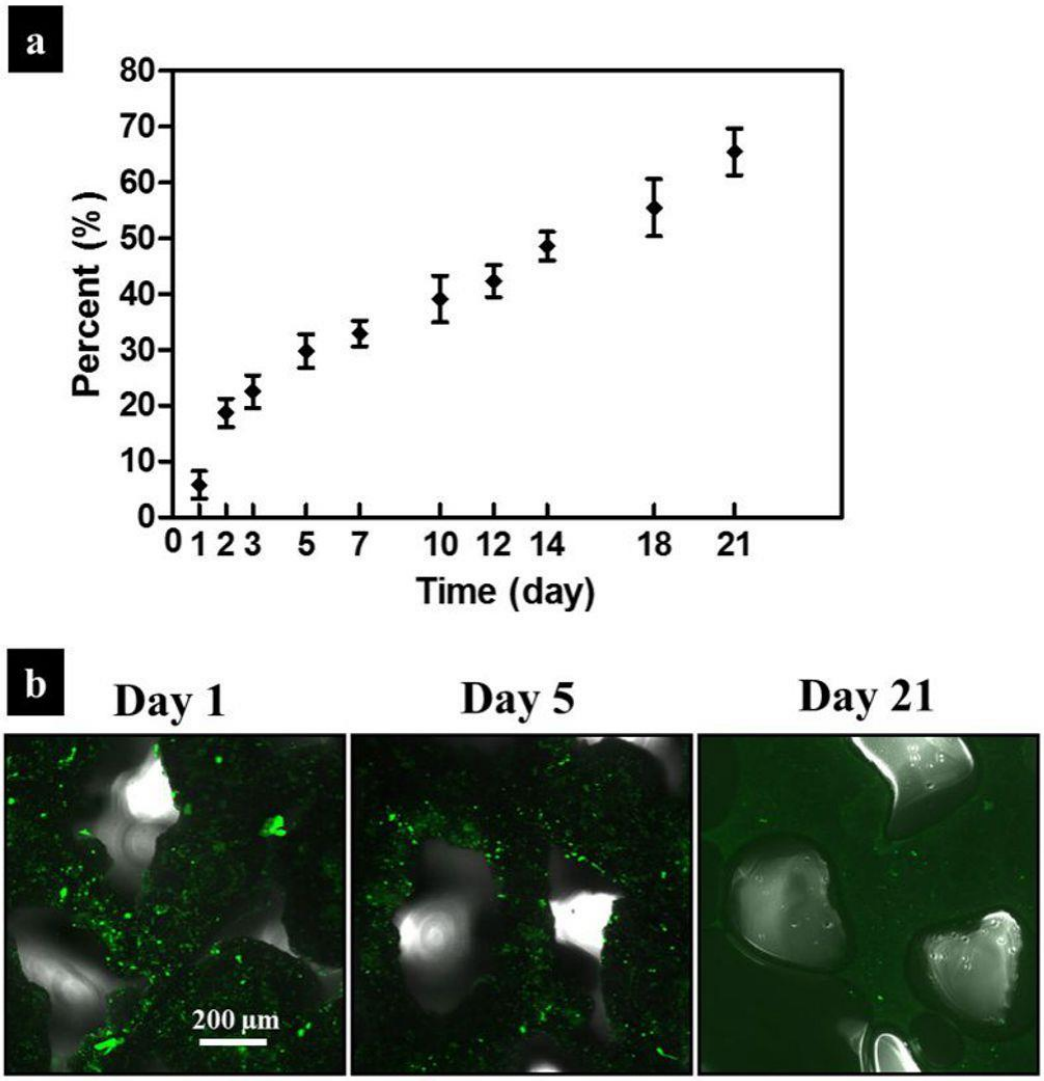

FIGURE 4 (a) BMP-2 release profile of conjugated recombinant human bone morphogenetic protein-2 (rhBMP-2) on collagen modified scaffold, HAp-B observed up to 21 days. (b) Immunofluorescence staining (BMP-2–FITC) analysis of BMP-2 present after 1, 5 and 21 days. BMP-2, bone morphogenetic protein2; FITC, fluorescein isothiocyanate; HAp, hydroxyapatite

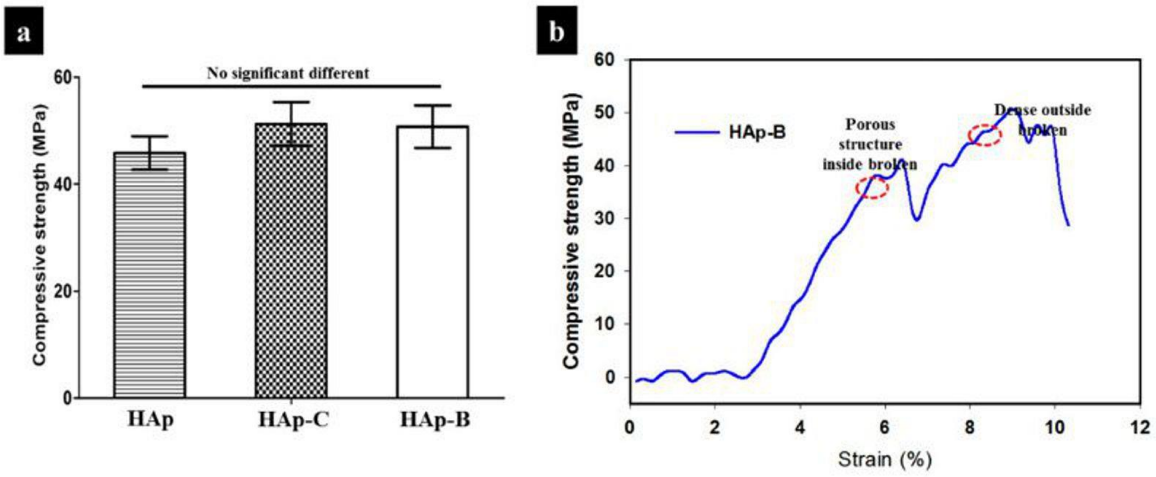

FIGURE 5 Mechanical property of the HAp-B scaffold showing compressive strength, with no significant difference at $p < .05$ compared with HAp and HAp-C scaffolds (a), and the inner and outer structural strength (b). HAp, hydroxyapatite

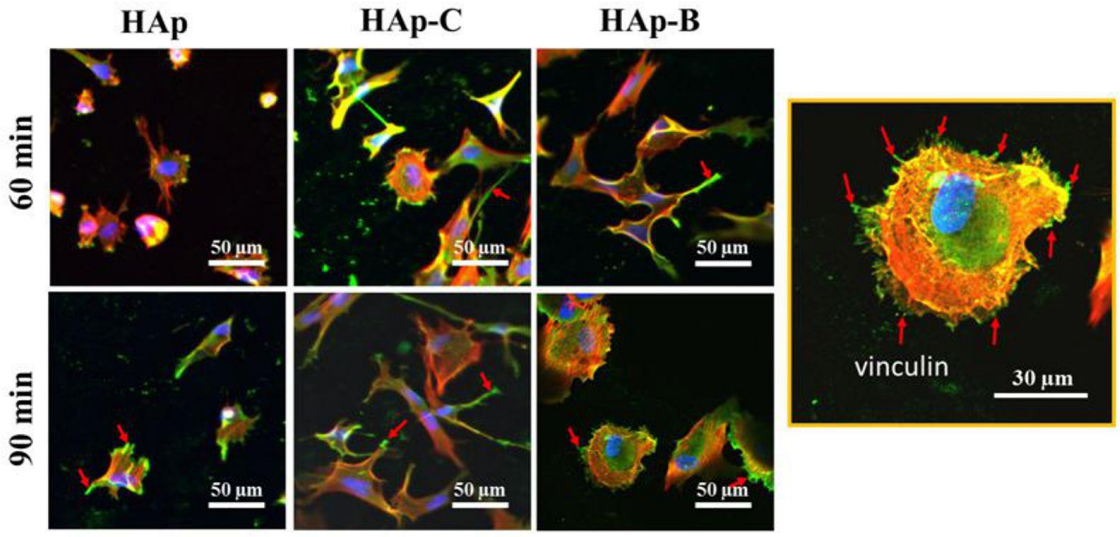

FIGURE 6 Vinculin distribution of hADSC on HAp, HAp-C, and HAp-B at 60- and 90-min incubation period by confocal microscopy. Vinculin (red arrow—green staining), F-actin (red staining), and nucleus (blue staining). hADSCs, human adipose-derived stem cells; HAp, hydroxyapatite

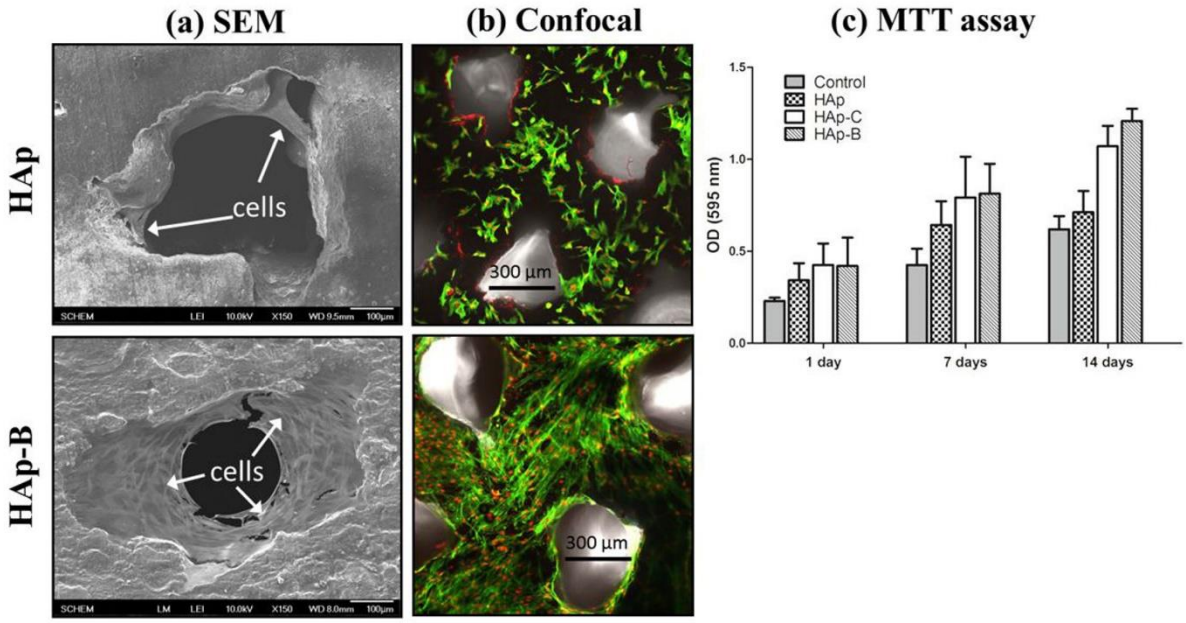

FIGURE 7 SEM (a) and confocal image (b) of hADSCs on HAp and HAp-B after 14 days of incubation. MTT assay showed cell viability at 1, 7, and 14 days on the surface of HAp, HAp-C, and HAp-B (c). hADSCs, human adipose-derived stem cells; HAp, hydroxyapatite; MTT, 3-(4,5-dimethylthiazol-2-yl)-2,5-diphenyltetrazolium bromide; SEM, scanning electron microscopy

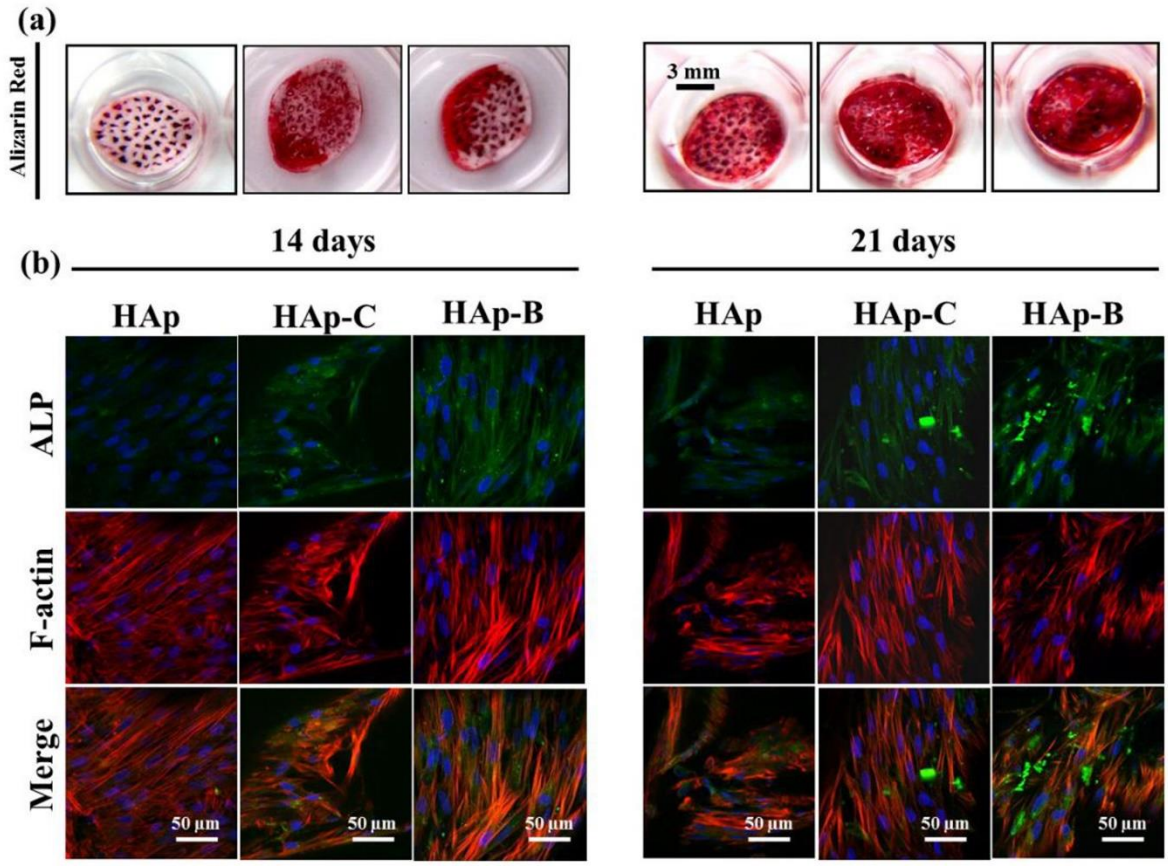

FIGURE 8 Alizarin red staining (a) and ALP immunofluorescence detection (b) of hADSCs cultured on HAp-C and HAp-B showing better expression than HAp after 14 and 21 days of incubation. ALP, alkaline phosphatase antibody; hADSCs, human adipose-derived stem cells; HAp, hydroxyapatite

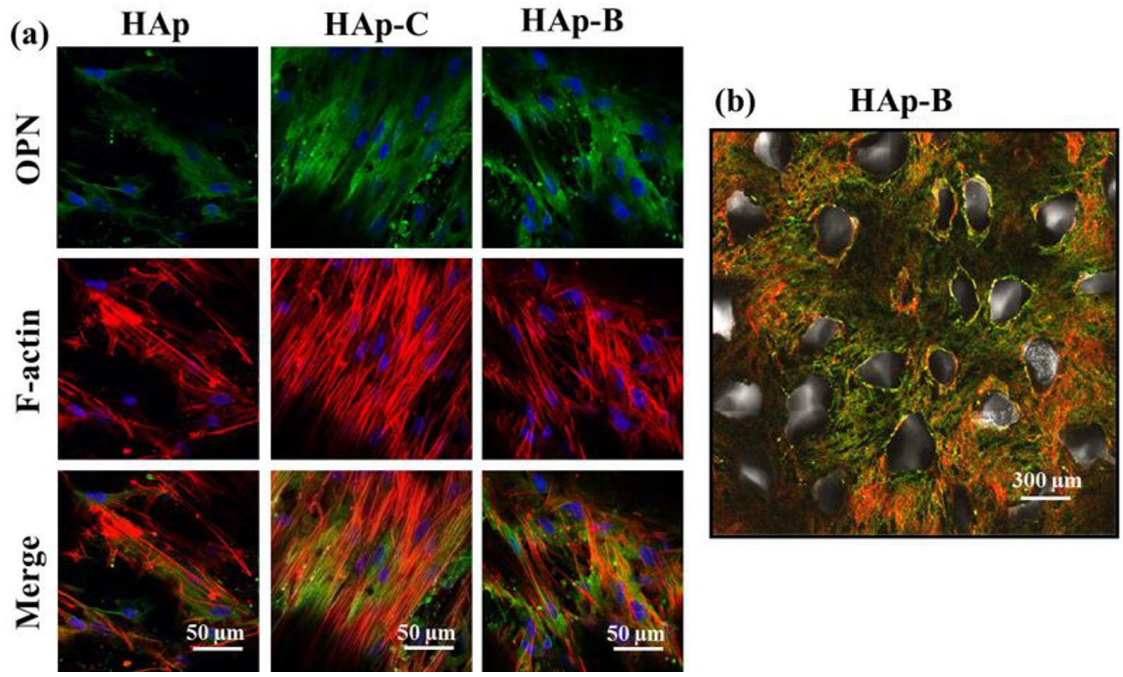

FIGURE 9 Confocal micrographs of hADSCs revealed a more prominent OPN expression (green) on HAp-C and HAp-B than HAp after 21 days of incubation. hADSCs, human adipose-derived stem cells; HAp, hydroxyapatite; OPN, osteopontin